

Ultrahigh-energy neutrino follow-up of gravitational wave events GW150914 and GW151226 with the Pierre Auger Observatory

A. Aab,¹ P. Abreu,² M. Aglietta,^{3,4} I. Al Samarai,⁵ I. F. M. Albuquerque,⁶ I. Allekotte,⁷ A. Almela,^{8,9} J. Alvarez Castillo,¹⁰ J. Alvarez-Muñiz,¹¹ M. Ambrosio,¹² G. A. Anastasi,¹³ L. Anchordoqui,¹⁴ B. Andrada,⁸ S. Andringa,² C. Aramo,¹² F. Arqueros,¹⁵ N. Arsene,¹⁶ H. Asorey,^{7,17} P. Assis,² J. Aublin,⁵ G. Avila,^{18,19} A. M. Badescu,²⁰ A. Balaceanu,²¹ R. J. Barreira Luz,² C. Baus,²² J. J. Beatty,²³ K. H. Becker,²⁴ J. A. Bellido,²⁵ C. Berat,²⁶ M. E. Bertaina,^{27,4} X. Bertou,⁷ P. L. Biermann,²⁸ P. Billoir,⁵ J. Biteau,²⁹ S. G. Blaess,²⁵ A. Blanco,² J. Blazek,³⁰ C. Bleve,^{31,32} M. Boháčová,³⁰ D. Boncioli,^{33,†} C. Bonifazi,³⁴ N. Borodai,³⁵ A. M. Botti,^{8,36} J. Brack,³⁷ I. Brancus,²¹ T. Bretz,³⁸ A. Bridgeman,³⁶ F. L. Briechle,³⁸ P. Buchholz,¹ A. Bueno,³⁹ S. Buitink,⁴⁰ M. Buscemi,^{41,42} K. S. Caballero-Mora,⁴³ L. Caccianiga,⁵ A. Cancio,^{9,8} F. Canfora,⁴⁰ L. Caramete,⁴⁴ R. Caruso,^{41,42} A. Castellina,^{3,4} G. Cataldi,³² L. Cazon,² R. Cester,^{27,4} A. G. Chavez,⁴⁵ J. A. Chinellato,⁴⁶ J. Chudoba,³⁰ R. W. Clay,²⁵ R. Colalillo,^{47,12} A. Coleman,⁴⁸ L. Collica,⁴ M. R. Coluccia,^{31,32} R. Conceição,² F. Contreras,^{18,19} M. J. Cooper,²⁵ S. Coutu,⁴⁸ C. E. Covault,⁴⁹ J. Cronin,⁵⁰ S. D'Amico,^{51,32} B. Daniel,⁴⁶ S. Dasso,^{52,53} K. Daumiller,³⁶ B. R. Dawson,²⁵ R. M. de Almeida,⁵⁴ S. J. de Jong,^{40,55} G. De Mauro,⁴⁰ J. R. T. de Mello Neto,³⁴ I. De Mitri,^{31,32} J. de Oliveira,⁵⁴ V. de Souza,⁵⁶ J. Debatin,³⁶ O. Deligny,²⁹ C. Di Giulio,^{57,58} A. Di Matteo,^{59,60} M. L. Díaz Castro,⁴⁶ F. Diogo,² C. Dobrigkeit,⁴⁶ J. C. D'Olive,¹⁰ A. Dorofeev,³⁷ R. C. dos Anjos,⁶¹ M. T. Dova,⁶² A. Dundovic,⁶³ J. Ebr,³⁰ R. Engel,³⁶ M. Erdmann,³⁸ M. Erfani,¹ C. O. Escobar,^{64,46} J. Espadanal,² A. Etchegoyen,^{8,9} H. Falcke,^{40,65,55} K. Fang,⁵⁰ G. Farrar,⁶⁶ A. C. Fauth,⁴⁶ N. Fazzini,⁶⁴ B. Fick,⁶⁷ J. M. Figueira,⁸ A. Filipčić,^{68,69} O. Fratu,²⁰ M. M. Freire,⁷⁰ T. Fujii,⁵⁰ A. Fuster,^{8,9} R. Gaior,⁵ B. García,⁷¹ D. Garcia-Pinto,¹⁵ F. Gaté,⁷² H. Gemmeke,⁷² A. Gherghel-Lascu,²¹ P. L. Ghia,⁵ U. Giaccari,³⁴ M. Giammarchi,⁷³ M. Giller,⁷⁴ D. Głás,⁷⁴ C. Glaser,³⁸ H. Glass,⁶⁴ G. Golup,⁷ M. Gómez Berisso,⁷ P. F. Gómez Vitale,^{18,19} N. González,^{8,36} B. Gookin,³⁷ A. Gorgi,^{3,4} P. Gorham,⁷⁵ P. Gouffon,⁶ A. F. Grillo,³³ T. D. Grubb,²⁵ F. Guarino,^{47,12} G. P. Guedes,⁷⁶ M. R. Hampel,⁸ P. Hansen,⁶² D. Harari,⁷ T. A. Harrison,²⁵ J. L. Harton,³⁷ Q. Hasankiadeh,⁷⁷ A. Haungs,³⁶ T. Hebbeker,³⁸ D. Heck,³⁶ P. Heimann,¹ A. E. Herve,²² G. C. Hill,²⁵ C. Hojvat,⁶⁴ E. Holt,^{36,8} P. Homola,³⁵ J. R. Hörandel,^{40,55} P. Horvath,⁷⁸ M. Hrabovský,⁷⁸ T. Huege,³⁶ J. Hulsman,^{8,36} A. Insolia,^{41,42} P. G. Isar,⁴⁴ I. Jandt,²⁴ S. Jansen,^{40,55} J. A. Johnsen,⁷⁹ M. Josebachuili,⁸ A. Kääpä,²⁴ O. Kambeitz,²² K. H. Kampert,²⁴ P. Kasper,⁶⁴ I. Katkov,²² B. Keilhauer,³⁶ E. Kemp,⁴⁶ J. Kemp,³⁸ R. M. Kieckhafer,⁶⁷ H. O. Klages,³⁶ M. Kleifges,⁷² J. Kleinfeller,¹⁸ R. Krause,³⁸ N. Krohm,²⁴ D. Kuempel,³⁸ G. Kukec Mezek,⁶⁹ N. Kunka,⁷² A. Kuotb Awad,³⁶ D. LaHurd,⁴⁹ M. Lauscher,³⁸ P. Lebrun,⁶⁴ R. Legumina,⁷⁴ M. A. Leigui de Oliveira,⁸⁰ A. Letessier-Selvon,⁵ I. Lhenry-Yvon,²⁹ K. Link,²² L. Lopes,² R. López,⁸¹ A. López Casado,¹¹ Q. Luce,²⁹ A. Lucero,^{8,9} M. Malacari,⁵⁰ M. Mallamaci,^{82,73} D. Mandat,³⁰ P. Mantsch,⁶⁴ A. G. Mariuzzi,⁶² I. C. Mariş,³⁹ G. Marsella,^{31,32} D. Martello,^{31,32} H. Martinez,⁸³ O. Martínez Bravo,⁸¹ J. J. Masías Meza,⁵³ H. J. Mathes,³⁶ S. Mathys,²⁴ J. Matthews,⁸⁴ J. A. J. Matthews,⁸⁵ G. Matthiae,^{57,58} E. Mayotte,²⁴ P. O. Mazur,⁶⁴ C. Medina,⁷⁹ G. Medina-Tanco,¹⁰ D. Melo,⁸ A. Menshikov,⁷² S. Messina,⁷⁷ M. I. Micheletti,⁷⁰ L. Middendorf,³⁸ I. A. Minaya,¹⁵ L. Miramonti,^{82,73} B. Mitrica,²¹ D. Mockler,²² L. Molina-Bueno,³⁹ S. Mollerach,⁷ F. Montanet,²⁶ C. Morello,^{3,4} M. Mostafá,⁴⁸ G. Müller,³⁸ M. A. Muller,^{46,86} S. Müller,^{36,8} I. Naranjo,⁷ L. Nellen,¹⁰ J. Neuser,²⁴ P. H. Nguyen,²⁵ M. Niculescu-Oglinzanu,²¹ M. Niechciol,¹ L. Niemietz,²⁴ T. Niggemann,³⁸ D. Nitz,⁶⁷ D. Nosek,⁸⁷ V. Novotny,⁸⁷ H. Nožka,⁷⁸ L. A. Núñez,¹⁷ L. Ochilo,¹ F. Oikonomou,⁴⁸ A. Olinto,⁵⁰ D. Pakk Selmi-Dei,⁴⁶ M. Palatka,³⁰ J. Pallotta,⁸⁸ P. Papenbreer,²⁴ G. Parente,¹¹ A. Parra,⁸¹ T. Paul,^{89,14} M. Pech,³⁰ F. Pedreira,¹¹ J. Pękala,³⁵ R. Pelayo,⁹⁰ J. Peña-Rodríguez,¹⁷ L. A. S. Pereira,⁴⁶ L. Perrone,^{31,32} C. Peters,³⁸ S. Petreara,^{59,13,60} J. Phuntsok,⁴⁸ R. Piegaiia,⁵³ T. Pierog,³⁶ P. Pieroni,⁵³ M. Pimenta,² V. Pirronello,^{41,42} M. Platino,⁸ M. Plum,³⁸ C. Porowski,²⁴ R. R. Prado,⁵⁶ P. Privitera,⁵⁰ M. Prouza,³⁰ E. J. Quel,⁸⁸ S. Quercfeld,²⁴ S. Quinn,⁴⁹ R. Ramos-Pollan,¹⁷ J. Rautenberg,²⁴ D. Ravnigani,⁸ D. Reinert,³⁸ B. Revenu,⁹¹ J. Ridky,³⁰ M. Risse,¹ P. Ristori,⁸⁸ V. Rizi,^{59,60} W. Rodrigues de Carvalho,⁶ G. Rodriguez Fernandez,^{57,58} J. Rodriguez Rojo,¹⁸ D. Rogozin,³⁶ M. Roth,³⁶ E. Roulet,⁷ A. C. Rovero,⁵² S. J. Saffi,²⁵ A. Saftoiu,²¹ H. Salazar,⁸¹ A. Saleh,⁶⁹ F. Salesa Greus,⁴⁸ G. Salina,⁵⁸ J. D. Sanabria Gomez,¹⁷ F. Sánchez,⁸ P. Sanchez-Lucas,³⁹ E. M. Santos,⁶ E. Santos,⁸ F. Sarazin,⁷⁹ B. Sarkar,²⁴ R. Sarmento,² C. A. Sarmiento,⁸ R. Sato,¹⁸ M. Schauer,²⁴ V. Scherini,^{31,32} H. Schieler,³⁶ M. Schimp,³⁶ D. Schmidt,^{36,8} O. Scholten,^{77,‡} P. Schovánek,³⁰ F. G. Schröder,³⁶ A. Schulz,³⁶ J. Schulz,⁴⁰ J. Schumacher,³⁸ S. J. Sciuotto,⁶² A. Segreto,^{92,42} M. Settimo,⁵ A. Shadkam,⁸⁴ R. C. Shellard,⁹³ G. Sigl,⁶³ G. Silli,^{8,36} O. Sima,¹⁶ A. Śmiałkowski,⁷⁴ R. Šmída,³⁶ G. R. Snow,⁹⁴ P. Sommers,⁴⁸ S. Sonntag,¹ J. Sorokin,²⁵ R. Squartini,¹⁸ D. Stanca,²¹ S. Stanić,⁶⁹ J. Stasielak,³⁵ P. Stassi,²⁶ F. Strafella,^{31,32} F. Suarez,^{8,9} M. Suarez Durán,¹⁷ T. Sudholz,²⁵ T. Suomijärvi,²⁹ A. D. Supanitsky,⁵² J. Swain,⁸⁹ Z. Szadkowski,⁷⁴ A. Taboada,²² O. A. Taborda,⁷ A. Tapia,⁸ V. M. Theodorou,⁴⁶ C. Timmermans,^{55,40} C. J. Todero Peixoto,⁹⁵ L. Tomankova,³⁶ B. Tomé,² G. Torralba Elipse,¹¹ D. Torres Machado,⁹⁶ M. Torri,⁸² P. Travnicek,³⁰ M. Trini,⁶⁹ R. Ulrich,³⁶ M. Unger,^{66,36} M. Urban,³⁸ J. F. Valdés Galicia,¹⁰ I. Valiño,¹¹ L. Valore,^{47,12} G. van Aar,⁴⁰ P. van Bodegom,²⁵ A. M. van den Berg,⁷⁷ A. van Vliet,⁴⁰ E. Varela,⁸¹ B. Vargas Cárdenas,¹⁰ G. Varner,⁷⁵ J. R. Vázquez,¹⁵ R. A. Vázquez,¹¹ D. Veberič,³⁶ I. D. Vergara Quispe,⁶² V. Verzi,⁵⁸ J. Vicha,³⁰ L. Villaseñor,⁴⁵ S. Vorobiov,⁶⁹ H. Wahlberg,⁶² O. Wainberg,^{8,9} D. Walz,³⁸ A. A. Watson,⁹⁷ M. Weber,⁷² A. Weindl,³⁶ L. Wiencke,⁷⁹ H. Wilczyński,³⁵ T. Winchen,²⁴ D. Wittkowski,²⁴ B. Wundheiler,⁸

S. Wykes,⁴⁰ L. Yang,⁶⁹ D. Yelos,^{9,8} A. Yushkov,⁸ E. Zas,¹¹ D. Zavrtanik,^{69,68} M. Zavrtanik,^{68,69} A. Zepeda,⁸³
 B. Zimmermann,⁷² M. Ziolkowski,¹ Z. Zong,²⁹ and F. Zuccarello^{41,42}
 (Pierre Auger Collaboration)*

- ¹*Universität Siegen, Fachbereich 7 Physik—Experimentelle Teilchenphysik, Siegen, Germany*
²*Laboratório de Instrumentação e Física Experimental de Partículas (LIP) and Instituto Superior Técnico (IST), Universidade de Lisboa (UL), Lisboa, Portugal*
³*Osservatorio Astrofisico di Torino (INAF), Torino, Italy*
⁴*INFN, Sezione di Torino, Torino, Italy*
⁵*Laboratoire de Physique Nucléaire et de Hautes Energies (LPNHE), Universités Paris 6 et Paris 7, CNRS-IN2P3, Paris, France*
⁶*Inst. de Física, São Paulo, Universidade de São Paulo, São Paulo, Brazil*
⁷*Centro Atómico Bariloche and Instituto Balseiro (CNEA-UNCuyo-CONICET), San Carlos de Bariloche, Argentina*
⁸*Instituto de Tecnologías en Detección y Astropartículas (CNEA, CONICET, UNSAM), Centro Atómico Constituyentes, Comisión Nacional de Energía Atómica, Buenos Aires, Argentina*
⁹*Facultad Regional Buenos Aires, Universidad Tecnológica Nacional, Buenos Aires, Argentina*
¹⁰*Universidad Nacional Autónoma de México, México, Distrito Federal, Mexico*
¹¹*Universidad de Santiago de Compostela, Santiago de Compostela, Spain*
¹²*INFN, Sezione di Napoli, Napoli, Italy*
¹³*Gran Sasso Science Institute (INFN), L'Aquila, Italy*
¹⁴*Department of Physics and Astronomy, Lehman College, City University of New York, Bronx, New York, USA*
¹⁵*Universidad Complutense de Madrid, Madrid, Spain*
¹⁶*Physics Department, University of Bucharest, Bucharest, Romania*
¹⁷*Universidad Industrial de Santander, Bucaramanga, Colombia*
¹⁸*Observatorio Pierre Auger, Malargüe, Mendoza, Argentina*
¹⁹*Observatorio Pierre Auger and Comisión Nacional de Energía Atómica, Malargüe, Mendoza, Argentina*
²⁰*University Politehnica of Bucharest, Bucharest, Romania*
²¹*“Horia Hulubei” National Institute for Physics and Nuclear Engineering, Bucharest-Magurele, Romania*
²²*Karlsruhe Institute of Technology, Institut für Experimentelle Kernphysik (IEKP), Karlsruhe, Germany*
²³*Ohio State University, Columbus, Ohio, USA*
²⁴*Department of Physics, Bergische Universität Wuppertal, Wuppertal, Germany*
²⁵*University of Adelaide, Adelaide, South Australia, Australia*
²⁶*Laboratoire de Physique Subatomique et de Cosmologie (LPSC), Université Grenoble-Alpes, CNRS/IN2P3, Grenoble, France*
²⁷*Università Torino, Dipartimento di Fisica, Torino, Italy*
²⁸*Max-Planck-Institut für Radioastronomie, Bonn, Germany*
²⁹*Institut de Physique Nucléaire d’Orsay (IPNO), Université Paris 11, CNRS-IN2P3, Orsay, France*
³⁰*Institute of Physics (FZU) of the Academy of Sciences of the Czech Republic, Prague, Czech Republic*
³¹*Università del Salento, Dipartimento di Matematica e Fisica “E. De Giorgi,” Lecce, Italy*
³²*INFN, Sezione di Lecce, Lecce, Italy*
³³*INFN Laboratori Nazionali del Gran Sasso, Assergi, Italy*
³⁴*Instituto de Física, Universidade Federal do Rio de Janeiro (UFRJ), Rio de Janeiro, Brazil*
³⁵*Institute of Nuclear Physics PAN, Krakow, Poland*
³⁶*Karlsruhe Institute of Technology, Institut für Kernphysik (IKP), Karlsruhe, Germany*
³⁷*Colorado State University, Fort Collins, Colorado, USA*
³⁸*RWTH Aachen University, III. Physikalisches Institut A, Aachen, Germany*
³⁹*Universidad de Granada and C.A.F.P.E., Granada, Spain*
⁴⁰*Institute for Mathematics, Astrophysics and Particle Physics (IMAPP), Radboud Universiteit, Nijmegen, Netherlands*
⁴¹*Università di Catania, Dipartimento di Fisica e Astronomia, Catania, Italy*
⁴²*INFN, Sezione di Catania, Catania, Italy*
⁴³*Universidad Autónoma de Chiapas, Tuxtla Gutiérrez, Chiapas, Mexico*
⁴⁴*Institute of Space Science, Bucharest-Magurele, Romania*
⁴⁵*Universidad Michoacana de San Nicolás de Hidalgo, Morelia, Michoacán, Mexico*
⁴⁶*Universidade Estadual de Campinas (UNICAMP), Campinas, Brazil*
⁴⁷*Dipartimento di Fisica “Ettore Pancini,” Università di Napoli “Federico II,” Napoli, Italy*
⁴⁸*Pennsylvania State University, University Park, Pennsylvania, USA*

- ⁴⁹Case Western Reserve University, Cleveland, Ohio, USA
- ⁵⁰University of Chicago, Chicago, Illinois, USA
- ⁵¹Dipartimento di Ingegneria, Università del Salento, Lecce, Italy
- ⁵²Instituto de Astronomía y Física del Espacio (IAFE, CONICET-UBA), Buenos Aires, Argentina
- ⁵³Departamento de Física and Departamento de Ciencias de la Atmósfera y los Océanos, FCEyN, Universidad de Buenos Aires, Buenos Aires, Argentina
- ⁵⁴Universidade Federal Fluminense, Volta Redonda, Brazil
- ⁵⁵Nationaal Instituut voor Kernfysica en Hoge Energie Fysica (NIKHEF), Science Park, Amsterdam, Netherlands
- ⁵⁶Universidade de São Paulo, São Carlos, Brazil
- ⁵⁷Dipartimento di Fisica, Università di Roma “Tor Vergata,” Roma, Italy
- ⁵⁸INFN, Sezione di Roma “Tor Vergata,” Roma, Italy
- ⁵⁹Dipartimento di Scienze Fisiche e Chimiche, Università dell’Aquila, L’Aquila, Italy
- ⁶⁰INFN, Gruppo Collegato dell’Aquila, L’Aquila, Italy
- ⁶¹Universidade Federal do Paraná, Setor Palotina, Brazil
- ⁶²IFLP, Universidad Nacional de La Plata and CONICET, La Plata, Argentina
- ⁶³Universität Hamburg, II. Institut für Theoretische Physik, Hamburg, Germany
- ⁶⁴Fermi National Accelerator Laboratory, Batavia, Illinois, USA
- ⁶⁵Stichting Astronomisch Onderzoek in Nederland (ASTRON), Dwingeloo, Netherlands
- ⁶⁶New York University, New York, New York, USA
- ⁶⁷Michigan Technological University, Houghton, Michigan, USA
- ⁶⁸Experimental Particle Physics Department, J. Stefan Institute, Ljubljana, Slovenia
- ⁶⁹Laboratory for Astroparticle Physics, University of Nova Gorica, Nova Gorica, Slovenia
- ⁷⁰Instituto de Física de Rosario (IFIR)—CONICET/U.N.R. and Facultad de Ciencias Bioquímicas y Farmacéuticas U.N.R., Rosario, Argentina
- ⁷¹Facultad Regional Mendoza (CONICET/CNEA), Instituto de Tecnologías en Detección y Astropartículas (CNEA, CONICET, UNSAM) and Universidad Tecnológica Nacional, Mendoza, Argentina
- ⁷²Karlsruhe Institute of Technology, Institut für Prozessdatenverarbeitung und Elektronik (IPE), Karlsruhe, Germany
- ⁷³INFN, Sezione di Milano, Milano, Italy
- ⁷⁴Faculty of Astrophysics, University of Łódź, Łódź, Poland
- ⁷⁵University of Hawaii, Honolulu, Hawaii, USA
- ⁷⁶Universidade Estadual de Feira de Santana (UEFS), Feira de Santana, Brazil
- ⁷⁷KVI—Center for Advanced Radiation Technology, University of Groningen, Groningen, Netherlands
- ⁷⁸Palacky University, RCPTM, Olomouc, Czech Republic
- ⁷⁹Colorado School of Mines, Golden, Colorado, USA
- ⁸⁰Universidade Federal do ABC (UFABC), Santo André, Brazil
- ⁸¹Benemérita Universidad Autónoma de Puebla (BUAP), Puebla, Mexico
- ⁸²Dipartimento di Fisica, Università di Milano, Milano, Italy
- ⁸³Centro de Investigación y de Estudios Avanzados del IPN (CINVESTAV), México, Distrito Federal, Mexico
- ⁸⁴Louisiana State University, Baton Rouge, Louisiana, USA
- ⁸⁵University of New Mexico, Albuquerque, New Mexico, USA
- ⁸⁶Universidade Federal de Pelotas, Pelotas, Brazil
- ⁸⁷Institute of Particle and Nuclear Physics, University Prague, Prague, Czech Republic
- ⁸⁸Centro de Investigaciones en Láseres y Aplicaciones, CITEDEF and CONICET, Buenos Aires, Argentina
- ⁸⁹Northeastern University, Boston, Massachusetts, USA
- ⁹⁰Unidad Profesional Interdisciplinaria en Ingeniería y Tecnologías Avanzadas del Instituto Politécnico Nacional (UPIITA-IPN), México, Distrito Federal, Mexico
- ⁹¹SUBATECH, École des Mines de Nantes, CNRS-IN2P3, Université de Nantes, Nantes, France
- ⁹²INAF—Istituto di Astrofisica Spaziale e Fisica Cosmica di Palermo, Palermo, Italy
- ⁹³Centro Brasileiro de Pesquisas Físicas (CBPF), Rio de Janeiro, Brazil
- ⁹⁴University of Nebraska, Lincoln, Nebraska, USA
- ⁹⁵Escola de Engenharia de Lorena, Universidade de São Paulo, Lorena, Brazil
- ⁹⁶Universidade Federal do Rio de Janeiro (UFRJ), Instituto de Física, Rio de Janeiro, Brazil
- ⁹⁷School of Physics and Astronomy, University of Leeds, Leeds, United Kingdom

(Received 26 August 2016; published 30 December 2016)

* auger_spokespersons@fnal.gov; <http://www.auger.org>

† Present address: Deutsches Elektronen-Synchrotron (DESY), Zeuthen, Germany.

‡ Also at Vrije Universiteit Brussels, Brussels, Belgium.

On September 14, 2015 the Advanced LIGO detectors observed their first gravitational wave (GW) transient GW150914. This was followed by a second GW event observed on December 26, 2015. Both events were inferred to have arisen from the merger of black holes in binary systems. Such a system may emit neutrinos if there are magnetic fields and disk debris remaining from the formation of the two black holes. With the surface detector array of the Pierre Auger Observatory we can search for neutrinos with energy E_ν above 100 PeV from pointlike sources across the sky with equatorial declination from about -65° to $+60^\circ$, and, in particular, from a fraction of the 90% confidence-level inferred positions in the sky of GW150914 and GW151226. A targeted search for highly inclined extensive air showers, produced either by interactions of downward-going neutrinos of all flavors in the atmosphere or by the decays of tau leptons originating from tau-neutrino interactions in the Earth's crust (Earth-skimming neutrinos), yielded no candidates in the Auger data collected within ± 500 s around or 1 day after the coordinated universal time (UTC) of GW150914 and GW151226, as well as in the same search periods relative to the UTC time of the GW candidate event LVT151012. From the nonobservation we constrain the amount of energy radiated in ultrahigh-energy neutrinos from such remarkable events.

DOI: [10.1103/PhysRevD.94.122007](https://doi.org/10.1103/PhysRevD.94.122007)

I. INTRODUCTION

On September 14, 2015 at 09:50:45 universal time (UTC) the Advanced LIGO detectors observed the first gravitational wave (GW) transient GW150914 [1]. The GW was inferred to have arisen from the merger of black holes in a binary system at a luminosity distance $D_s = 410_{-180}^{+160}$ Mpc. The estimated amount of energy released in the form of gravitational waves was $E_{\text{GW}} = 3.0_{-0.5}^{+0.5} M_\odot c^2$ solar masses [1,2]. A second GW event GW151226 [3] was detected at 03:38:53 UTC on December 26, 2015, also inferred to be produced by the merger of two black holes at a distance $D_s = 440_{-190}^{+180}$ Mpc. In this case the amount of energy released in the form of GW was $E_{\text{GW}} = 1.0_{-0.2}^{+0.1} M_\odot c^2$ [3]. A third candidate event, LVT151012, was observed on October 12, 2015 at 09:54:43 UTC. Although LVT151012 is consistent with a binary black-hole merger it is not significant enough to claim an unambiguous detection [4].

The observation of GW events with LIGO has motivated several models on the production of electromagnetic counterparts to GW in binary black-hole mergers [5,6]. Moreover, observations with the Fermi GBM detector have revealed the presence of a transient source above 50 keV, only 0.4 s after GW150914, with localization consistent with its direction [7] and with a possible association with a short gamma-ray burst [8–10]. On the other hand, other gamma-ray and x-ray observatories did not find any potential counterpart either for GW150914 [11–14] or for GW151226 [15].

Mergers of black holes are a potential environment where cosmic rays can be accelerated to ultrahigh energies (UHEs) provided there are magnetic fields and disk debris remaining from the formation of the black holes [10,16]. These are two necessary ingredients to accelerate cosmic rays to ultrahigh energies through the Fermi mechanism at astrophysical sources (see for instance [17]). The estimated

rate of this type of mergers can account for the total energy observed in ultrahigh-energy cosmic rays (UHECRs) and their distribution in the sky [16]. The UHE cosmic rays can interact with the surrounding matter or radiation to produce ultrahigh-energy gamma rays and neutrinos [10,16]. Other models speculate on the possibility that protons could be accelerated up to ~ 10 EeV energies in a one-shot boost [18]. Collisions of UHE protons with photon backgrounds and gas surrounding the black hole would produce UHE neutrinos. The remarkable power of GW150914 could produce a proton spectrum peaked at EeV energies with a lesser emission of neutrinos in the PeV energy range [18]. Neutrino experiments with peak sensitivities in the TeV–PeV energy range such as IceCube and ANTARES have reported no neutrino candidates in spatial and temporal coincidence with GW150914 [19].

With the surface detector (SD) of the Pierre Auger Observatory [20] we can identify neutrino-induced air showers in the energy range above 100 PeV [21]. Showers induced by neutrinos at large zenith angles can start their development deep in the atmosphere so that they have a considerable amount of electromagnetic component at the ground (“young” shower front). On the other hand, at large zenith angles the atmosphere is thick enough that the electromagnetic component of the more numerous nucleonic cosmic rays, which interact shortly after entering the atmosphere, gets absorbed and the shower front at ground level is dominated by muons (“old” shower front). The SD consists of 1660 water-Cherenkov stations spread over an area of ~ 3000 km², separated by 1.5 km and arranged in a triangular grid. Although the SD is not separately sensitive to the muonic and electromagnetic components of the shower, nor to the depth at which the shower is initiated, the signals produced by the passage of shower particles, digitized with 25 ns time resolution [20], allow us to distinguish narrow traces in time induced by inclined showers initiated high in the atmosphere, from the broad

signals expected in inclined showers initiated close to the ground. Applying this simple idea, with the SD of the Pierre Auger Observatory [20] we can efficiently detect inclined showers and search for two types of neutrino-induced showers at energies above 100 PeV.

- (i) Earth-skimming (ES) showers induced by tau neutrinos (ν_τ) that travel in a slightly upward direction. A ν_τ can skim the Earth's crust and interact near the surface, inducing a tau lepton that escapes the Earth and decays in flight in the atmosphere, close to the SD. Typically, only ν_τ -induced showers with zenith angles $90^\circ < \theta < 95^\circ$ may be identified.
- (ii) Showers initiated by neutrinos of any flavor moving down at large zenith angles $75^\circ < \theta < 90^\circ$ with respect to the vertical and that interact in the atmosphere close to the surface-detector array through charged-current or neutral-current interactions. These are referred to as downward-going high zenith angle (DGH) neutrinos.

In previous publications [21–24] methods were established to identify inclined and deeply initiated showers with the SD of the Pierre Auger Observatory. These were applied blindly to search for ES and DGH neutrinos in the data collected with the SD up to June 20, 2013. No neutrino candidate was found. As a result an upper limit to the diffuse flux of UHE neutrinos (i.e., from an ensemble of unresolved sources) was obtained in [21]. Also the same analysis was applied to place upper limits on continuous (in time) pointlike sources of UHE neutrinos [25].

In this paper we use the same identification criteria as in [21] to search for neutrinos in temporal and spatial coincidence with GW150914 and GW151226, as well as with the GW candidate event LVT151012 [4]. The search was performed within ± 500 s around the time of either GW event as well as in the period of 1 day after their occurrence. The choice of these two rather broad time windows is motivated by the association of mergers of compact systems and gamma-ray bursts (GRBs) [8,9,26]. The ± 500 s window [27] corresponds to an upper limit on the duration of the prompt phase of GRBs, when typically PeV neutrinos are thought to be produced in interactions of accelerated cosmic rays and the gamma rays within the GRB itself. The choice of the 1-day window after the GW event is a conservative upper limit on the duration of GRB afterglows, where ultrahigh-energy neutrinos are thought to be produced in interactions of UHECRs with the lower-energy photons of the GRB afterglow (see [26] for a review).

The results of the search allow us to set constraints on the emission of UHE neutrinos from the merger of two black holes. These constraints apply in the energy range [~ 100 PeV, ~ 25 EeV] and are complementary to those of IceCube/ANTARES [19], which apply in the energy range [~ 100 GeV, ~ 100 PeV].

II. RESULTS

The neutrino identification criteria applied to data collected with the Pierre Auger Observatory are summarized in Ref. [21]. First, inclined showers are selected in the different angular ranges of the ES and DGH channels. Secondly, deeply penetrating showers are identified in the inclined-event sample through the broad time structure of the signals expected to be induced in the water-Cherenkov SD stations indicative of the presence of an electromagnetic component [21].

The sensitivity to UHE neutrinos in Auger is limited to large zenith angles. As a consequence at each instant in time, neutrinos can be detected efficiently only from a specific portion of the sky. A source at declination δ and right ascension α (in equatorial coordinates) is seen at the latitude of Auger ($\lambda = -35.2^\circ$) and at a given sidereal time t with a zenith angle $\theta(t)$ given by

$$\cos \theta(t) = \sin \lambda \sin \delta + \cos \lambda \cos \delta \sin(2\pi t/T - \alpha), \quad (1)$$

where T is the duration of one sidereal day. From Eq. (1) it is straightforward to calculate the fraction of a sidereal day a source at declination δ is visible in the ES angular range ($90^\circ, 95^\circ$) and in the DGH one ($75^\circ, 90^\circ$). In Fig. 1 we show two sky maps in equatorial coordinates where the color scale indicates the fraction of a sidereal day during which each declination is seen in the ES (top plot) and DGH (bottom plot) field of view. The positions of GW150914 and GW151226 are not well constrained by data collected with the Advanced LIGO detectors but 90% C.L. contours are provided and are also shown in Fig. 1. At 90% C.L. the declination of the source of GW150914 can be between $\delta \sim -1.0^\circ$ and $\sim -14.5^\circ$ or between $\delta \sim -38.5^\circ$ and $\sim -78.0^\circ$, and that of GW151226 between $\delta \sim -72.7^\circ$ and $\sim 60.9^\circ$ as can be seen in Fig. 1. Both 90% C.L. declination ranges overlap with the field of view of the ES and DGH channels for fractions of one sidereal day that can reach up to $\sim 17\%$ and $\sim 35\%$, respectively. If the emission took less time than a day these numbers could change significantly, depending on the sky position of the GW event relative to Auger during the emission time. The overlapping between the Auger field of view in the inclined directions and the 90% C.L. contour position of the GW event is larger for GW151226 as seen in Fig. 1 and also for LVT151012.

A. Searching for UHE neutrinos in coincidence with GW events

We searched for neutrino events in coincidence with GW150914, GW151226, and LVT151012 in two periods of time: ± 500 s around the UTC times at which they occurred, as well as in a period of 1 day after GW150914, GW151226, and LVT151012.

The performance of the SD array is monitored every minute and is rather stable in each of the ± 500 s and 1 day

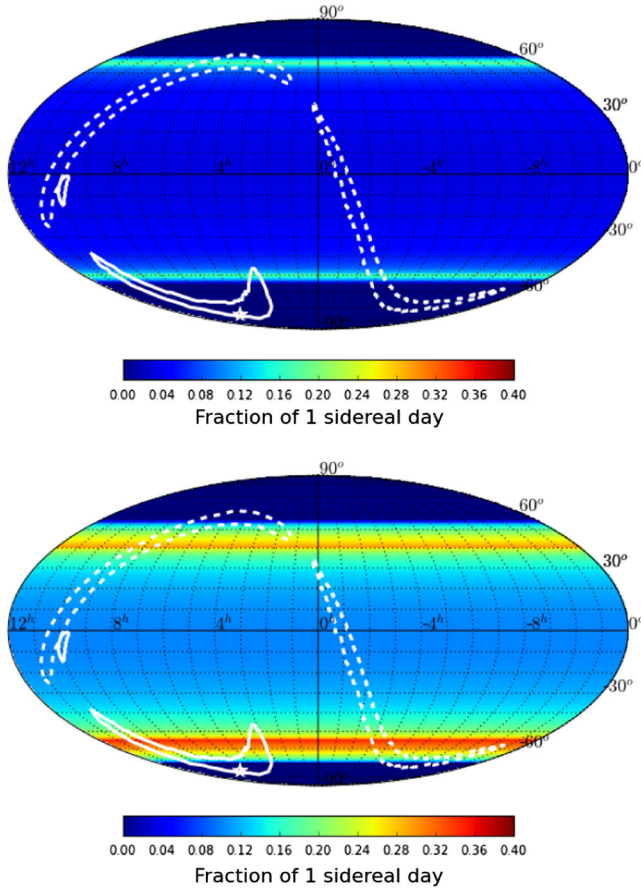


FIG. 1. Sky map in equatorial coordinates where the color scale indicates the fraction of one sidereal day for which a pointlike source at declination δ is visible to the SD of the Auger Observatory (latitude $\lambda = -35.2^\circ$) at zenith angle $90^\circ < \theta < 95^\circ$ (top panel), and $75^\circ < \theta < 90^\circ$ (bottom panel). The white solid lines indicate the 90% C.L. contour position of GW150914 [1,2] and the dashed white lines indicate the corresponding 90% C.L. contour position of GW151226 [3,4]. The white star indicates the best-fit position of the GW150914 event obtained in combination with data from the Fermi-GBM instrument (see Fig. 10 in [7]).

periods of time after either GW event. The average (root-mean squared) number of active stations during the search periods of the GW150914 and GW151226 events and of the LVT151012 candidate amount, respectively, to $\sim 97.5\%$ ($\sim 1.5\%$), $\sim 95.6\%$ ($\sim 5.5\%$), and $\sim 94.0\%$ (6.5%) of the total number of stations in the SD array.

The arrival directions of cosmic rays are determined in Auger from the relative arrival times of the shower front in the triggered stations. The angular accuracy depends on the number of triggered stations, on the energy and on the zenith angle of the shower. Studies of cosmic-ray-induced showers below 80° zenith angle have revealed that the angular resolution is better than 2.5° , improving significantly as the number of triggered stations increases [28,29]. Similar results are expected for neutrino-induced showers.

Unfortunately the field of view of the ES channel did not overlap within ± 500 s of the time of coalescence of

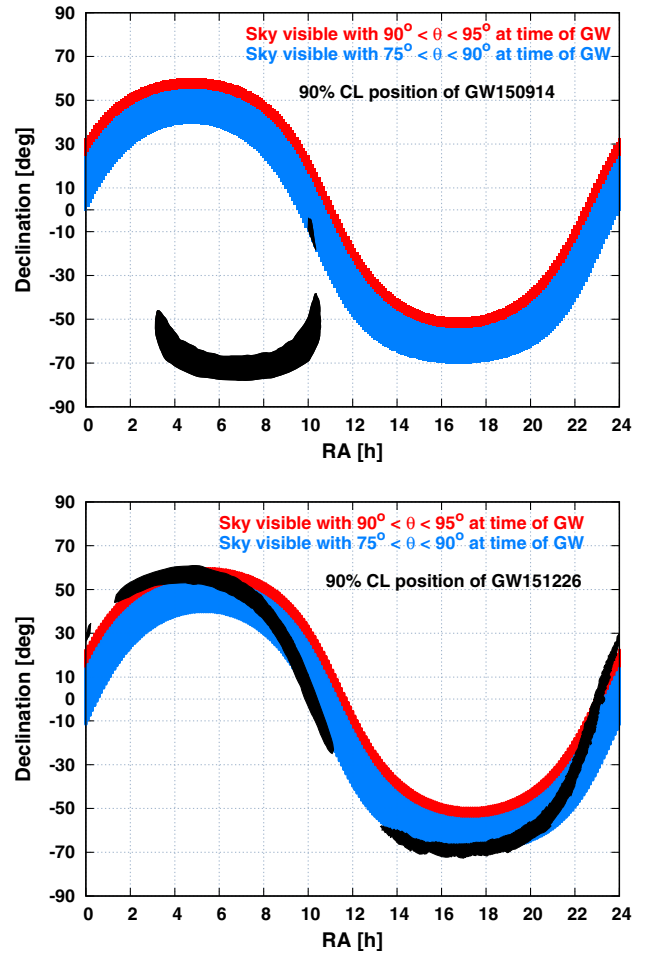


FIG. 2. Instantaneous field of view of the ES (red band) and DGH (blue band) channels at the moment of coalescence of GW150914 (top panel) and of GW151226 (bottom panel). The black spots represent the 90% C.L. contour enclosing the positions of the corresponding GW events. Note that by chance the instantaneous field of view of Auger is approximately the same at the instants of occurrence of both GW events.

event GW150914 with the 90% C.L. contour enclosing its position; see the top panel of Fig. 2. However there is a significant overlap in the case of GW151226 as can be seen in the bottom panel of Fig. 2 and also in the case of LVT151012. Also GW150914, GW151226, and LVT151012 are visible in the DGH angular range $75^\circ < \theta < 90^\circ$ within ± 500 s of occurrence—see Fig. 2. In all cases a significant portion of the inferred position of the source is visible for a fraction of the time in 1 day after the corresponding GW event, as the Earth rotates and the field of view of the ES and DGH analyses moves through the sky (see Fig. 1).

The search for UHE neutrinos in Auger data produced the following results:

- (i) No inclined showers passing the ES or DGH selection were found in the time window ± 500 s around GW150914 or GW151226.

- (ii) A total of 24 inclined showers were found with the ES selection criteria, 12 in each of the 1 day periods after GW150914 and GW151226 events, but none of them fulfilled the neutrino identification criteria. Also 24 and 22 inclined showers were found with the DGH selection 1 day after GW150914 and GW151226, respectively, with none of them identified as a neutrino candidate. All selected inclined events have properties compatible with background nucleonic cosmic-ray events.
- (iii) Also, no neutrino candidates were found within ± 500 s around or 1 day after the UTC time of the GW candidate event LVT151012 [4].

B. Constraints on the sources of GW

The absence of neutrino candidates allows us to place upper limits to the UHE neutrino flux from GW150914 and GW151226 (in the following we restrict ourselves to the two confirmed GW events) as a function of equatorial declination δ . The expected number of events for a neutrino flux $dN^{\text{GW}}/dE_\nu(E_\nu)$ from a pointlike source at declination δ is given by

$$N_{\text{event}}^{\text{GW}} = \int_{E_\nu} \frac{dN_\nu^{\text{GW}}}{dE_\nu}(E_\nu) \mathcal{E}_{\text{GW}}(E_\nu, \delta) dE_\nu, \quad (2)$$

where $\mathcal{E}_{\text{GW}}(E_\nu, \delta)$ is the effective exposure to a pointlike flux of UHE neutrinos as a function of neutrino energy E_ν and declination. For each channel ES and DGH we calculate the exposure to UHE neutrinos $\mathcal{E}^{\text{ES}}(E_\nu, \delta)$ and $\mathcal{E}^{\text{DGH}}(E_\nu, \delta)$, respectively, following the procedure explained in [21–25]. The exposure is obtained by integrating the SD aperture (area \times solid angle) over the search period T_{search} , multiplied by the neutrino cross section for each neutrino channel, and weighted by the selection and detection efficiency obtained from Monte Carlo simulations [21]. When integrating over the search period, we only consider the fraction of time when the source is visible from the SD of Auger within the zenith angle range of the corresponding neutrino selection. In each of the search periods the performance of the SD array was very stable; in particular, there were no large periods of inactivity as confirmed using the continuous monitoring of the Auger SD array.

Assuming a standard E_ν^{-2} energy dependence for a constant UHE neutrino flux per flavor from the source of GW150914 or GW151226, namely, $dN_\nu^{\text{GW}}/dE_\nu = k^{\text{GW}} E_\nu^{-2}$, a 90% C.L. upper limit on k^{GW} can be obtained as

$$k^{\text{GW}}(\delta) = \frac{2.39}{\int_{E_\nu} E_\nu^{-2} \mathcal{E}_{\text{GW}}(E_\nu, \delta) dE_\nu}. \quad (3)$$

We applied Eq. (3) to obtain upper limits to the normalization of the flux $k_{\text{ES}}^{\text{GW}}(\delta)$ and $k_{\text{DGH}}^{\text{GW}}(\delta)$ in each channel. The

combined upper limit to the normalization $k^{\text{GW}}(\delta)$ of the flux is obtained as $(k^{\text{GW}})^{-1} = (k_{\text{ES}}^{\text{GW}})^{-1} + (k_{\text{DGH}}^{\text{GW}})^{-1}$.

Systematic uncertainties are incorporated in the upper limit in Eq. (3) and were taken into account using a semi-Bayesian extension [30] of the Feldman and Cousins approach [31] (see Table II in [21] for a detailed account of the main sources of systematic uncertainties).

From the limits to the flux normalization we obtained upper limits to the UHE neutrino spectral fluence radiated per flavor in a similar fashion to those obtained in [19],

$$E_\nu^2 \frac{dN_\nu}{dE_\nu} \times T_{\text{search}} = k^{\text{GW}}(\delta) T_{\text{search}}, \quad (4)$$

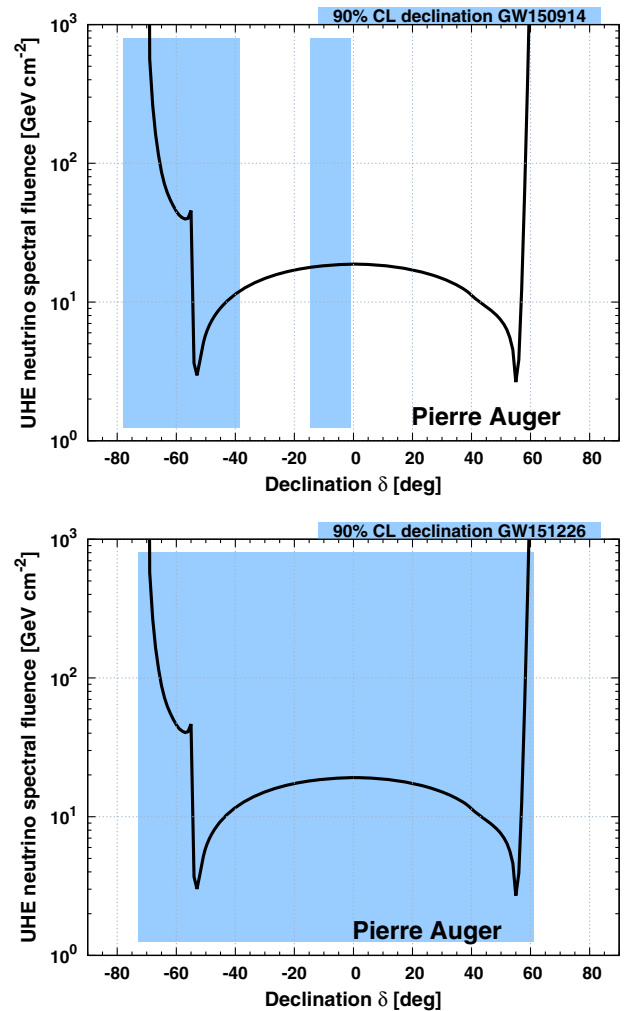


FIG. 3. Top panel: Upper limits to the UHE neutrino spectral fluence per flavor [see Eq. (4)] from the source of GW150914 as a function of equatorial declination δ . Fluences above the black solid line are excluded at 90% C.L. from the nonobservation of UHE neutrino events in Auger. The 90% C.L. declination bands of the GW150914 are indicated in the plot by the shaded rectangles. Bottom panel: Same as the top panel for the GW event GW151226.

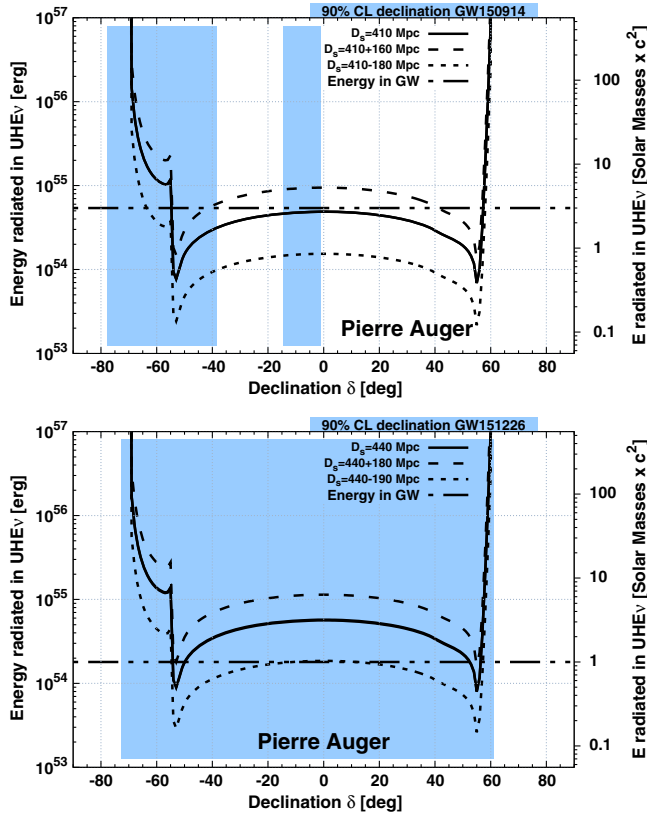


FIG. 4. Top panel: Constraints on $E_{\nu,\text{tot}}$ the energy radiated in UHE neutrinos (per flavor) from the source of GW150914 as a function of equatorial declination δ . Energies above the black solid line, assuming the luminosity distance to the source is $D_s = 410$ Mpc, are excluded at the 90% C.L. from the non-observation of UHE neutrinos in Auger. The long-dashed line represents the constraints if the source is farther away at $D_s = 410 + 160$ Mpc, and the short-dashed line if the source is closer to Earth at $D_s = 410 - 180$ Mpc corresponding to the 90% C.L. interval of possible distances to the source. For reference the dot-dashed black horizontal line represents $E_{\text{GW}} \approx 5.4 \times 10^{54}$ erg, the inferred energy radiated in gravitational waves from GW150914 [1,2]. The 90% C.L. declination bands of the GW150914 are indicated in the plot by the shaded rectangles. Bottom panel: Same as the top panel for GW151226 but in this case $D_s = 440_{-190}^{+180}$ Mpc and the energy released in the form of GW is $E_{\text{GW}} \approx 1.8 \times 10^{54}$ erg.

where $T_{\text{search}} = 1 \text{ day} + 500 \text{ s}$ is the total search period interval. Here it is assumed that the sources of GW events emit UHE neutrinos continuously during the search period. The constraints on spectral fluence are shown in Fig. 3 and depend strongly on the source direction. The dependence is mainly driven by the fraction of the time a source at declination δ is within the field of view of the ES and DGH analyses. The upper limit to the fluence is dominated by the intrinsically larger sensitivity of the ES analysis to UHE neutrinos at energies above 100 PeV. The constraints on the spectral fluence are above 3 GeV cm^{-2} and are very similar for both GW150914 and GW151226 as shown in Fig. 3,

since the performance and number of active water-Cherenkov stations of the SD array are equally stable in each of the 1-day periods of time after each GW event.

Assuming that the radiated spectrum has a E_ν^{-2} dependence on neutrino energy above $E_\nu = 100 \text{ PeV}$ [17], the corresponding upper limit to the total fluence is obtained by integrating the spectral fluence over the interval. Finally, it is straightforward to obtain constraints on the total energy radiated in neutrinos $E_{\nu,\text{tot}}(\delta)$ assuming the source is located at a luminosity distance D_s , $E_{\nu,\text{tot}}(\delta) = \mathcal{F}_\nu(\delta) \times 4\pi D_s^2$. These constraints are shown in Fig. 4.

The most restrictive upper limits on the total energy emitted per flavor in UHE neutrinos are achieved at declination $\delta \sim -53^\circ$

$$E_{\nu,\text{tot}}(\delta = -53^\circ) < 7.7 \times 10^{53} \text{ erg}, \quad \text{for GW150914} \quad (5)$$

and at $\delta \sim 55^\circ$

$$E_{\nu,\text{tot}}(\delta = 55^\circ) < 7.9 \times 10^{53} \text{ erg}, \quad \text{for GW151226.} \quad (6)$$

The constraints on total energy can be expressed as fractions f_ν of energy in UHE neutrinos $E_{\nu,\text{tot}}$ relative to the energy radiated in gravitational waves E_{GW} . The most stringent upper limit on the fraction f_ν of energy radiated in UHE neutrinos relative to the energy emitted in GW150914 is

$$f_\nu(\delta = -53^\circ) < 14.3\% \quad \text{for GW150914,} \quad (7)$$

assuming the source is located at the central value of the 90% C.L. interval of distances $D_s = 410$ Mpc. This fraction changes from $\sim 4.5\%$ to $\sim 27.6\%$ as the source distance varies between the lower and upper limits of the 90% C.L. interval $D_s = (230, 570)$ Mpc quoted in [1].

For the case of GW151226 since the total energy released in the GW is three times smaller the corresponding best upper limit on f_ν is

$$f_\nu(\delta = 55^\circ) < 44.1\% \quad \text{for GW151226,} \quad (8)$$

assuming the source is located at $D_s = 440$ Mpc.

III. DISCUSSION

The results in this work represent the first upper limits on UHE neutrino emission from an identified source of GW—the merger of two black holes—and the first follow-up of GW events with neutrinos of energies above 100 PeV.

The upper limits on fluence emitted in the form of UHE neutrinos are strongly declination dependent. With the SD of the Pierre Auger Observatory we are sensitive to a large fraction of the declination range in which the sources of GW150914 and GW151226 could be located at the 90% C.L. as shown in Fig. 1.

While our most stringent upper limit to the total energy in the form of UHE neutrinos for the GW150914 event is $\sim 7.7 \times 10^{53}$ erg per flavor at $\delta_0 = -53^\circ$, the IceCube/ANTARES best upper limit ($\nu_\mu + \bar{\nu}_\mu$) is $\sim 5.4 \times 10^{51}$ erg at declinations close to the equator [19]. However, the IceCube/ANTARES limits apply in the energy range [100 GeV, 100 PeV] while the Auger limits apply in the complementary energy range [100 PeV, 25 EeV].

In [16] it was argued that black-hole mergers would have sufficient luminosity to power the acceleration of cosmic rays up to 100 EeV. With a modest efficiency $\lesssim 0.03$ per GW event per unit of gravitational wave energy release radiated in the form of UHECRs and given the inferred rate of black-hole mergers [4], a source population of this type could achieve the energy budget needed to explain the observed UHECRs [16]. In this work we place a most stringent upper limit on the fraction of GW energy channeled into neutrinos of $\sim 14\%$. If only 3% of the energy of the GW is channeled into UHECRs [16], and the same energy goes into UHE neutrinos, then we would expect at most on the order of 0.5 events in Auger in coincidence with GW150914.

An upper bound to the diffuse single-flavor neutrino flux integrated over a source population of this type was estimated also in [16],

$$E_\nu^2 \frac{dN_\nu}{dE_\nu} \Big|_{\text{diffuse}}^{\text{theory}} \lesssim (1.5 - 6.9) \times 10^{-8} \text{ GeV cm}^{-2} \text{ s}^{-1} \text{ sr}^{-1}, \quad (9)$$

depending on the evolution with redshift of the sources and assuming an optical depth $\tau = 1$ to neutrino production in the debris surrounding the black-hole mergers. This upper bound is a factor between ~ 3 and 10 above the limit to the diffuse flux of UHE neutrinos obtained with Auger data up to June 20, 2013 in [21], namely,

$$E_\nu^2 \frac{dN_\nu}{dE_\nu} \Big|_{\text{diffuse}}^{\text{Auger}} < 6.4 \times 10^{-9} \text{ GeV cm}^{-2} \text{ s}^{-1} \text{ sr}^{-1}. \quad (10)$$

It is possible that there are no significant fluxes of UHE neutrinos associated with the coalescence of black holes; more phenomenological work in this area is needed. In the case that cosmic rays are indeed accelerated as suggested in [16], our constraints on the diffuse flux of UHE neutrinos would imply that (1) the optical depth to neutrino production is significantly smaller than 1 as expected in GRB models; (2) only a fraction of the luminosity that can be extracted from the black hole can be invested in UHECR acceleration; (3) only a fraction of the energy of the protons goes into charged pions (that are the parents of the neutrinos); or (4) a combination of the three possibilities.

The Advanced LIGO-Virgo detection of GW150914 and GW151226 represents a breakthrough in our understanding of the Universe. Similar analyses to those presented in this work will be important to provide constraints on the progenitors of the GW emission. Given the inferred rate of events $9\text{--}240 \text{ Gpc}^{-3} \text{ yr}^{-1}$ [4] new GW events can be

expected in the near future, closer to Earth and/or more energetic, and/or produced by another type of source that is more likely to accelerate UHECRs and produce UHE neutrinos than the merger of two black holes, such as for instance binary neutron-star mergers, and core-collapse supernovae with rapidly rotating cores [32,33].

Finally, the detection of UHE neutrino candidates in Auger in coincidence with GW events could help in pinpointing the position of the source of GW with an accuracy that depends on the shower zenith angle and energy, ranging from less than ~ 1 deg² to order 10 deg² in the least favorable cases. This is to be compared with the currently known position of the two GW events, namely, a few 100 deg². Observations with Auger can significantly constrain the position of the source and help the follow-up of the GW events with optical and other observatories of electromagnetic radiation. This is an example where multi-messenger observations (GW, neutrinos, and photons) can reveal properties of the sources which may not be discerned from one type of signal alone.

ACKNOWLEDGMENTS

The successful installation, commissioning, and operation of the Pierre Auger Observatory would not have been possible without the strong commitment and effort from the technical and administrative staff in Malargüe. We are very grateful to the following agencies and organizations for financial support. Comisión Nacional de Energía Atómica, Agencia Nacional de Promoción Científica y Tecnológica (ANPCyT), Consejo Nacional de Investigaciones Científicas y Técnicas (CONICET), Gobierno de la Provincia de Mendoza, Municipalidad de Malargüe, NDM Holdings, and Valle Las Leñas, in gratitude for their continuing cooperation over land access, Argentina; the Australian Research Council; Conselho Nacional de Desenvolvimento Científico e Tecnológico (CNPq), Financiadora de Estudos e Projetos (FINEP), Fundação de Amparo à Pesquisa do Estado de Rio de Janeiro (FAPERJ), São Paulo Research Foundation (FAPESP) Grants No. 2010/07359-6 and No. 1999/05404-3, Ministério de Ciência e Tecnologia (MCT), Brazil, Grants No. MSMT CR LG15014, No. LO1305, and No. LM2015038; the Czech Science Foundation Grant No. 14-17501S, Czech Republic; Centre de Calcul IN2P3/CNRS, Centre National de la Recherche Scientifique (CNRS), Conseil Régional Ile-de-France, Département Physique Nucléaire et Corpusculaire (PNC-IN2P3/CNRS), Département Sciences de l'Univers (SDU-INSU/CNRS), Institut Lagrange de Paris (ILP) Grant No. LABEX ANR-10-LABX-63, within the Investissements d'Avenir Programme Grant No. ANR-11-IDEX-0004-02, France; Bundesministerium für Bildung und Forschung (BMBF), Deutsche Forschungsgemeinschaft (DFG), Finanzministerium Baden-Württemberg, Helmholtz Alliance for Astroparticle Physics (HAP), Helmholtz-

Gemeinschaft Deutscher Forschungszentren (HGF), Ministerium für Wissenschaft und Forschung, Nordrhein Westfalen, Ministerium für Wissenschaft, Forschung und Kunst, Baden-Württemberg, Germany; Istituto Nazionale di Fisica Nucleare (INFN), Istituto Nazionale di Astrofisica (INAF), Ministero dell’Istruzione, dell’Università e della Ricerca (MIUR), Gran Sasso Center for Astroparticle Physics (CFA), CETEMPS Center of Excellence, Ministero degli Affari Esteri (MAE), Italy; Consejo Nacional de Ciencia y Tecnología (CONACYT) Grant No. 167733, Mexico; Universidad Nacional Autónoma de México (UNAM), Grant No. PAPIIT DGAPA-UNAM, Mexico; Ministerie van Onderwijs, Cultuur en Wetenschap, Nederlandse Organisatie voor Wetenschappelijk Onderzoek (NWO), Stichting voor Fundamenteel Onderzoek der Materie (FOM), Netherlands; National Centre for Research and Development, Grants No. ERA-NET-ASPERA/01/11 and No. ERA-NET-ASPERA/02/11, National Science Centre, Grants No. 2013/08/M/ST9/00322, No. 2013/08/M/ST9/00728 and No. HARMONIA 5–2013/10/M/ST9/

00062, Poland; Portuguese national funds and FEDER funds within Programa Operacional Factores de Competitividade through Fundação para a Ciência e a Tecnologia (COMPETE), Portugal; Romanian Authority for Scientific Research ANCS, CNDI-UEFISCDI partnership projects Grants No. 20/2012, No. 194/2012, and No. PN 16 42 01 02; Slovenian Research Agency, Slovenia; Comunidad de Madrid, Fondo Europeo de Desarrollo Regional (FEDER) funds, Ministerio de Economía y Competitividad, Xunta de Galicia, European Community 7th Framework Program, Grant No. FP7-PEOPLE-2012-IEF-328826, Spain; Science and Technology Facilities Council, United Kingdom; Department of Energy, Contracts No. DE-AC02-07CH11359, No. DE-FR02-04ER41300, No. DE-FG02-99ER41107, and No. DE-SC0011689; National Science Foundation, Grant No. 0450696; the Grainger Foundation, USA; NAFOSTED, Vietnam; Marie Curie-IRSES/EPLANET, European Particle Physics Latin American Network, European Union 7th Framework Program, Grant No. PIRSES-2009-GA-246806; and UNESCO.

-
- [1] B. P. Abbott *et al.* (LIGO Scientific and Virgo Collaborations), *Phys. Rev. Lett.* **116**, 061102 (2016).
- [2] B. P. Abbott *et al.* (LIGO Scientific and Virgo Collaborations), *Phys. Rev. Lett.* **116**, 241102 (2016).
- [3] B. P. Abbott *et al.* (LIGO Scientific and Virgo Collaborations), *Phys. Rev. Lett.* **116**, 241103 (2016).
- [4] B. P. Abbott *et al.* (LIGO Scientific and Virgo Collaborations), *Phys. Rev. X* **6**, 041015 (2016).
- [5] I. Bartos, B. Kocsis, Z. Haiman, and S. Márka, arXiv:1602.03831v2.
- [6] N. C. Stone, B. D. Metzger, and Z. Haiman, *Mon. Not. R. Astron. Soc.* **464**, 946 (2017).
- [7] V. Connaughton *et al.*, *Astrophys. J. Lett.* **826**, L6 (2016).
- [8] R. Moharana, S. Razzaque, N. Gupta, and P. Mészáros, *Phys. Rev. D* **93**, 123011 (2016).
- [9] R. Perna, D. Lazzati, and B. Giacomazzo, *Astrophys. J. Lett.* **821**, L18 (2016).
- [10] K. Murase, K. Kashiyama, P. Mészáros, I. Shoemaker, and N. Senno, *Astrophys. J. Lett.* **822**, L9 (2016).
- [11] V. Savchenko *et al.* (INTEGRAL Collaboration), *Astrophys. J. Lett.* **820**, L36 (2016).
- [12] M. Ackerman *et al.* (Fermi-LAT Collaboration), *Astrophys. J. Lett.* **823**, L2 (2016).
- [13] E. Troja, A. M. Read, A. Tiengo, and R. Salvaterra, *Astrophys. J. Lett.* **822**, L8 (2016).
- [14] M. Tavani *et al.* (AGILE Collaboration), *Astrophys. J. Lett.* **825**, L4 (2016).
- [15] J. L. Racusin *et al.* (Fermi-LAT & Fermi-GBM Collaborations), arXiv:1606.04901 [Astrophys. J. (to be published)].
- [16] K. Kotera and J. Silk, *Astrophys. J. Lett.* **823**, L29 (2016).
- [17] T. K. Gaisser, F. Halzen, and T. Stanev, *Phys. Rep.* **258**, 173 (1995).
- [18] L. A. Anchordoqui, *Phys. Rev. D* **94**, 023010 (2016).
- [19] S. Adrián-Martínez *et al.* (LIGO & Virgo, IceCube, and ANTARES Collaborations), *Phys. Rev. D* **93**, 122010 (2016).
- [20] A. Aab *et al.* (Pierre Auger Collaboration), *Nucl. Instrum. Methods Phys. Res., Sect. A* **798**, 172 (2015).
- [21] A. Aab *et al.* (Pierre Auger Collaboration), *Phys. Rev. D* **91**, 092008 (2015).
- [22] P. Abreu *et al.* (Pierre Auger Collaboration), *Phys. Rev. D* **84**, 122005 (2011).
- [23] J. Abraham *et al.* (Pierre Auger Collaboration), *Phys. Rev. Lett.* **100**, 211101 (2008).
- [24] J. Abraham *et al.* (Pierre Auger Collaboration), *Phys. Rev. D* **79**, 102001 (2009).
- [25] P. Abreu *et al.* (Pierre Auger Collaboration), *Astrophys. J. Lett.* **755**, L4 (2012).
- [26] P. Mészáros, *Rep. Prog. Phys.* **69**, 2259 (2006).
- [27] B. Baret *et al.*, *Astropart. Phys.* **35**, 1 (2011).
- [28] C. Bonifazi for the Pierre Auger Collaboration, *Nucl. Phys. B, Proc. Suppl.* **190**, 20 (2009).
- [29] A. Aab *et al.* (Pierre Auger Collaboration) *J. Cosmol. Astropart. Phys.* **08** (2014) 019.
- [30] J. Conrad, O. Botner, A. Hallgren, and C. Pérez de los Heros, *Phys. Rev. D* **67**, 012002 (2003).
- [31] G. J. Feldman and R. D. Cousins, *Phys. Rev. D* **57**, 3873 (1998).
- [32] I. Bartos, P. Brady, and S. Márka, *Classical Quantum Gravity* **30**, 123001 (2013).
- [33] S. Ando *et al.*, *Rev. Mod. Phys.* **85**, 1401 (2013).